Determination of the fine-structure properties of the $2p$ subshell of atomic chlorine

S. B. Whitfield,[1] S. Hallman,[2] M. O. Krause,[2] C. D. Caldwell,[3] and R. D. Cowan[4]
[1]*Department of Physics and Astronomy, University of Wisconsin–Eau Claire, Eau Claire, Wisconsin 54702*
[2]*Department of Physics, University of Central Florida, Orlando, Florida 32816*
[3]*National Science Foundation, 4201 Wilson Boulevard, Arlington, Virginia 22230*
[4]*Los Alamos National Laboratory, Los Alamos, New Mexico 87545*
(Received 1 April 1999)

A measurement of the fine-structure properties of the atomic chlorine $2p$ subshell has been carried out using electron spectrometry in conjunction with synchrotron radiation. We observe eight of the ten photopeaks predicted for this open-shell atom. Binding energies, relative intensities, and angular distribution parameters are reported for an incident photon energy of 245 eV. Experimental binding energies and intensities are in reasonable agreement with our calculations using a Slater-Condon superposition-of-configuration method. [S1050-2947(99)50309-0]

PACS number(s): 32.80.Fb, 32.80.Hd

The utilization of electron spectrometry in conjunction with synchrotron radiation has engendered a continuing interest in the study of the dynamics of the process of photoionization of atoms for nearly 30 years. Yet despite this rich history [1–4], the vast majority of experimental work has focused on the rare gases, which comprise a very small portion of the Periodic Table. This is largely due to the experimental ease of using the rare gases as an atomic target. However, if one wishes to focus on the role of electron correlation in the dynamics of the photoionization process, a study of open-shell systems is far better suited. This is primarily due to the nonspherical nature of the ground state of the open-shell atom. While there has been a fair degree of synchrotron based electron spectrometry involving the valence shells of some open-shell atoms produced by the evaporative heating of metallic solids [3,5], there has been only a handful of experiments done on the halogens [6–9], owing chiefly to the difficulty in producing a usable atomic beam. The halogens, by virtue of being one electron short of a filled p subshell, provide one of the simplest proving grounds for theoretical studies of the photoionization dynamics of open-shell atoms.

Recently [8], we investigated the $2p \rightarrow ns,md$ excitations in atomic chlorine by way of total ion-yield measurements. Concurrent calculations predicted ten $2p$ thresholds. However, a direct determination of their energies was not possible experimentally because no discernible Rydberg series exist. In order to compare theory with experiment, a different experimental method must be used. Photoelectron spectrometry is ideally suited to this task as it allows a direct determination of the energies of these thresholds.

In this paper we report on a measurement of the $2p$-subshell photoionization of atomic chlorine and concurrent calculations. The experiment was carried out on a bending-magnet beamline at the Aladdin storage ring in Stoughton, Wisconsin, on the HERMON monochromator [10]. The experimental setup utilizes a microwave discharge tube to dissociate a suitable molecule, in this case HCl, into its constituent atoms. In addition, Ar was added to help stabilize the discharge. Based on previous measurements under similar conditions [6], we do not expect the population of excited states in the discharge to be greater than 5%. A more detailed description of the experimental setup can be found in Refs. [9,11]. In the dipole approximation, the electron intensity $I_i(\theta)$ of the photoelectrons ejected at an angle θ with respect to the polarization vector of the synchrotron radiation is given by

$$I_i(\theta) \propto \frac{d\sigma_i}{d\Omega} = \frac{\sigma_i}{4\pi}\left(1 + \frac{\beta_i}{4}(1 + 3p\cos 2\theta)\right). \qquad (1)$$

Here $d\sigma_i/d\Omega$ is the partial differential cross section for the emission of an electron from the subshell i, σ_i is the partial cross section, β_i the angular distribution parameter, and p the degree of linear polarization of the photon beam. By determining the ratio of the electron intensity at the two extreme angles, $\theta = 0°$ and 90°, β can be determined, provided the polarization is known. We found $p = 0.89(2)$. Relative partial cross sections were found by recording the electron intensity at the magic angle $\theta_m = 0.5\cos^{-1}(-1/3p)$, where the spectra are free of angular distribution effects. They can also be found by solving Eq. (1) for σ_i and using the derived β values and the electron intensity recorded at either 0° or 90°. The total resolution inherent in our spectra, including contributions from the analyzer, the photon beam, and the natural width of the observed lines, was 350 meV.

To protect the integrity of the monochromator from the reactive target gases, the interaction region was separated from the monochromator's exit mirror by a 120-nm carbon filter with a transmission of about 92% at a photon energy of 245 eV. Calibration of the photon energy was done by comparing the difference in kinetic energies of the Kr-$3d_{5/2}$ photopeak and the Kr $N_3 - M_{4,5}M_{4,5}$ ($^1S_0$) Auger line, yielding $h\nu = 245.04(3)$ eV. An additional calibration was performed at a nominal photon energy of 280 eV using Ar-$2p$ photopeaks and their resulting Auger lines. From this calibration set the binding energies of the HCl-$2p$ photopeaks (used to establish the binding energies of the Cl-$2p$ photopeaks), also recorded at a photon energy of 280 eV, were determined. We found $E_b(2p_{3/2}) = 207.401(39)$ eV and

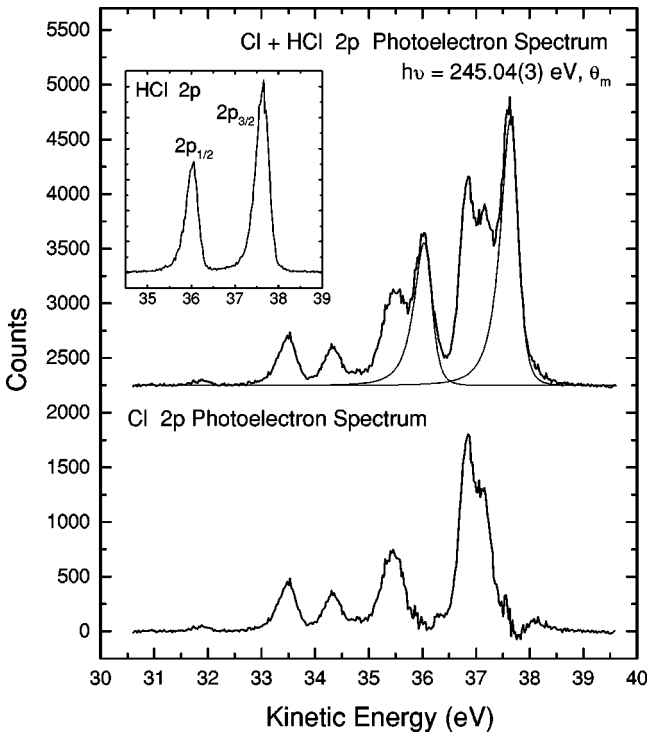

FIG. 1. Discharge-on PES of the Cl + HCl $2p$ photopeaks (upper part). The step size is 25 meV. The underlying HCl-$2p$ photopeaks, thin lines, are also shown. Discharge-off PES (inset). The Cl-$2p$ PES resulting from the subtraction of the fitted HCl-$2p$ peaks (lower part).

$E_b(2p_{1/2}) = 209.012(39)$ eV, in excellent agreement with the values of Shaw *et al.* [12].

Figure 1 illustrates the basic procedure used in obtaining an HCl-free atomic chlorine photoelectron spectrum (PES). In contrast to earlier studies [6,8,9], obtaining an HCl-free PES by subtraction of the discharge-on PES from the discharge-off PES proved difficult for the following reasons. First, the HCl-$2p$ photopeaks and the Cl-$2p$ photopeaks are strongly overlapping, making it difficult to determine the appropriate normalization factor between the two spectra. Second, we observed a broadening of the width of the photopeaks in the discharge-on PES as compared to the discharge-off PES due to small changes in the source volume potential with the discharge running. Without correctly accounting for this broadening, significant error would be introduced into the subtraction process. As a result, the following procedure was followed. First, a fit of the postcollision interaction (PCI) [13] distorted HCl-$2p$ photopeaks (inset of Fig. 1) was done using a distorted Pearson-7 function [14]. Then, the entire discharge-on PES was fit with symmetric Pearson-7 functions for the Cl-$2p$ lines [15] and distorted Pearson-7 functions for the two HCl-$2p$ lines where the degree of asymmetry was *fixed* to be the same as in the discharge-off spectrum. The upper part of Fig. 1 shows the transmission corrected Cl + HCl discharge-on PES with the fitted profiles of the HCl-$2p$ photopeaks. Subtraction of the fitted HCl-$2p$ photopeaks from the discharge-on PES yields an HCl-free PES, the lower PES in Fig. 1. While the fitted HCl-$2p$ profile does not entirely account for all of the HCl-$2p$ photopeaks in the region around 38 eV, we do not expect this to introduce significant error into our final analysis.

The ground-state configuration of atomic chlorine is $1s^2 2s^2 2p^6 3s^2 3p^5 (^2P_{3/2})$. Following the removal of a $2p$ electron, there are ten terms that can arise from coupling the $2p^5$ subshell with the $3p^5$ subshell: $^1S_0$, $^3S_1$, $^1P_1$, $^3P_0$, $^3P_1$, $^3P_2$, $^1D_2$, $^3D_1$, $^3D_2$, and $^3D_3$. All of these correspond to allowed ionic states because, when coupled to an εs ($^2S_{1/2}$) or an εd ($^2D_{3/2,5/2}$) continuum electron, the dipole selection rules $^2P_{3/2} \rightarrow {}^2S_{1/2}$, $^2P_{1/2,3/2}$, $^2D_{3/2,5/2}$ are satisfied.

Binding energies of the ten different terms were calculated using a Slater-Condon superposition-of-configuration method [16]. To assess the effects of configuration interaction (CI) on the computed values, several different calculations were performed. The first were single-configuration calculations for the ground configurations of the atom and the ion. Then calculations were done for both atom and ion, including configurations corresponding to a $3p$ to $4p$ excitation and $3s$ to $3d$, $4d$, and $5d$ excitations. The only excitation of importance was that from $3s$ to $3d$, and so for simplicity all further calculations included only the ground configurations and the excited configurations $2p^6 3s 3p^5 3d$ for the atom and $2p^5 3s 3p^5 3d$ for the ion. The perturbations were larger for the ion than for the atom, resulting in downward shifts in each computed threshold energy by amounts averaging about 0.4 eV. Calculations of the level displacements from configuration centers of gravity were made using Coulomb scaling factors of 0.85, 0.90, and 0.95 to approximate the effects of neglected small CI effects. The best agreement with experiment was seen for a scaling factor of 0.90, and this was used for final results. (This differs from the value 0.80 used earlier [8].)

We also calculated weighted bound-free oscillator strengths (gf), per Rydberg width of continuum, for transitions from $2p^6 3s^2 3p^5 + 2p^6 3s 3p^5 3d$ to $(2p^5 3s^2 3p^5 + 2p^5 3s 3p^5 3d)\varepsilon s, \varepsilon d$, using an average kinetic energy of the εs or εd electron of 35 eV (see Fig. 1); values for transitions from the ground level of the atom were then summed over all final states corresponding to each ion-core level. Calculations were made using Coulomb scaling factors of 0.85 to 0.95; differences in summed oscillator strengths were minor, and in all cases were less than 2% of the value for the strongest transition (that for the $^3D_3$ threshold).

The upper panel of Fig. 2 shows the Cl-$2p$ PES from Fig. 1 converted to a binding-energy scale, including the overall fit and its decomposition. In the lower panel the predicted theoretical PES and its decomposition are shown. The peak full width at half maximum (FWHM) and shape were set to match the values obtained from the fit of the data. The LS designation of each photopeak is also given. Note that the theoretical PES has not been shifted in any way. In Table I we list both the experimental and theoretical binding energies and relative intensities that are made with respect to peak 7, since this peak is the most clearly resolved peak of appreciable intensity. The experimental relative intensities are an average of the values determined at the magic angle, and those derived from the 0° PES using the measured β values. Both sets of measurements yielded results within 8% of each other, except for peaks 1 and 2 where the disagreement is up to 14%. The assignments of the peaks, in both LSJ and jj coupling, are also given based on their correspondence to the theoretical PES.

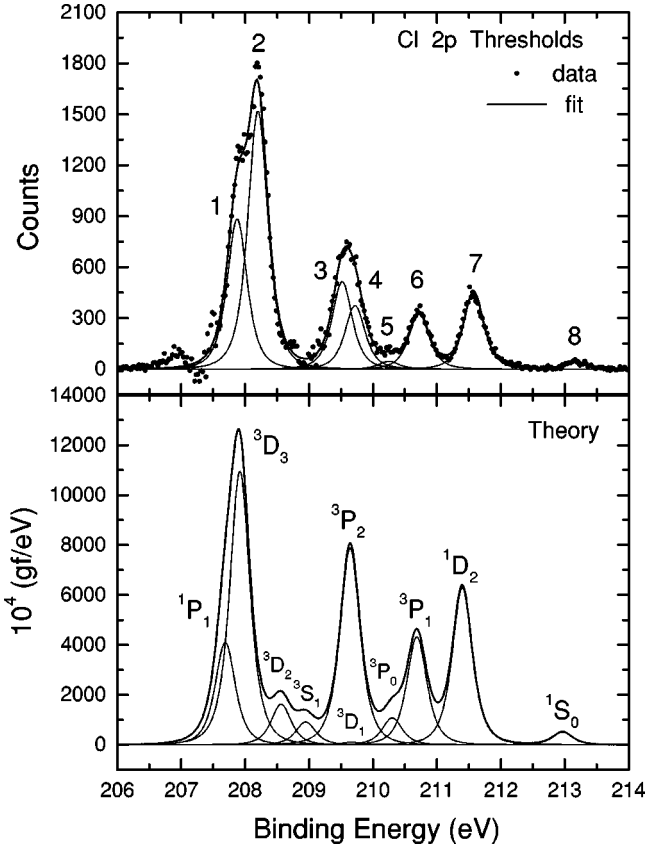

FIG. 2. The Cl-2p photoelectron PES from Fig. 1 indicating the fit and its decomposition into eight peaks of equal width (upper part). The theoretical PES including the *LSJ* assignments of each peak (lower part). Note: the $^3D_1$ peak is barely visible below the $^3P_2$ line.

Comparing experiment and theory we find good qualitative agreement and considerable quantitative agreement. The major discrepancies are (i) the relative intensity and splitting of peaks 1 and 2 and their combined intensity in comparison to the rest of the PES, (ii) the apparent lack of peaks in the experimental PES between lines 2 and 3, and (iii) where theory predicts one large peak, $^3P_2$, two are deduced from the fit of the data (peaks 3 and 4).

With regard to point (i), a difference in binding energy between peaks 1 and 2 is found to be 0.326(30) eV, while theory gives 0.224 eV. Here it would be difficult to argue that the splitting should be smaller because a shoulder, peak 1, is clearly seen in the data, even with the presence of the unsubtracted HCl lines (see Fig. 1). This argument also applies to the relative intensity between these two lines, which would appear to be underestimated by theory. While experiment clearly indicates a larger intensity imparted to these lines than theory, we cannot rule out that we overcorrected for transmission effects or did not subtract out all of the residual HCl-2p photopeaks, and thereby exaggerated the intensity of these Cl peaks. In any case, discrepancies are probably no greater than to be expected from the limited accuracy of the present theoretical method.

For point (ii), no definitive conclusions can be drawn. The region between peaks 2 and 3 corresponds to the location of the subtracted HCl-2$p_{1/2}$ photopeak. Because this region is so sensitive to the subtraction process, it is possible that these peaks are present in our PES but were subtracted out along with the HCl line. In fact, a closer inspection of the bottom PES in Fig. 1 indicates the presence of a small shoulder between a kinetic energy of 36.0 and 36.5 eV, which could be the $^3D_2$ line.

With respect to point (iii), our experimental resolution and HCl subtraction procedure does not allow us to rule out the possibility that peaks 3 and 4 could be combined into one peak. It should be mentioned that the fit was carried out assuming that the FWHM of *all* peaks is the same. This in general, need not be true, particularly for inner-shell photoionization of open-shell atoms. This was demonstrated theoretically in the Auger decay of Ar^+, where a clear difference in the widths of the Auger multiplet terms was found [17]. We expect the natural width of the Cl-2p photo peaks to be about the same as those of the autoionizing $2p^5 3s^2 ns,md$ states [8]. Calculated widths of these autoionizing states are generally on the order of 20 meV, but could be as high as 120 meV in some cases. As our resolution is about 350 meV, it is almost entirely due to the analyzer and the photon beam. This makes it unlikely that we could observe any real difference in the natural widths of these photopeaks, even if some have natural widths as large as 120 meV.

TABLE I. Binding energies, relative intensities, and β values of the chlorine 2p photopeaks observed at 245.04(3) eV.

Peak	Binding energy (eV)		ΔE (eV)		Relative intensity (%)			Assignment	
number	Experiment	Theory	Expt.-Theor.	$10^4 gf$	Expt.	Theor.	β	*LSJ*	*jj*
1	207.850(15)	207.694	+0.156	1867	190(10)	65.2	1.16(15)	$^1P_1$	$(\frac{3}{2},\frac{3}{2})_1$
2	208.176(15)	207.918	+0.258	4985	300(40)	174	1.06(15)	$^3D_3$	$(\frac{3}{2},\frac{3}{2})_3$
		208.560		738		25.8		$^3D_2$	$(\frac{3}{2},\frac{1}{2})_2$
3 [a]	209.457(15)	208.946	+0.511	415	110(6)	14.5	1.00(15)	$^3S_1$	$(\frac{3}{2},\frac{1}{2})_1$
4 [a]	209.683(15)	209.642	+0.041	3585	81(5)	125	1.46(15)	$^3P_2$	$(\frac{3}{2},\frac{3}{2})_2$
		209.665		47		1.64		$^3D_1$	$(\frac{1}{2},\frac{1}{2})_1$
5	210.189(15)	210.298	−0.109	489	10(2)	17.1	1.32(15)	$^3P_0$	$(\frac{3}{2},\frac{3}{2})_0$
6	210.688(10)	210.685	+0.003	1966	73(5)	68.6	1.16(10)	$^3P_1$	$(\frac{1}{2},\frac{3}{2})_1$
7	211.548(10)	211.399	+0.149	2864	100	100	1.10(10)	$^1D_2$	$(\frac{1}{2},\frac{3}{2})_2$
8	213.147(15)	212.964	+0.183	232	8(1)	8.10	0.52(10)	$^1S_0$	$(\frac{1}{2},\frac{1}{2})_0$

[a]Peaks 3 and 4 could be one peak corresponding to the $^3P_2$ line.

The β values derived from our spectra recorded at $\theta = 0°$ and 90° are listed in Table I. With the exception of peak 8, there is not a large variation in the β values among the photopeaks. This result may initially seem somewhat surprising. However, since the β value of each photoline is principally determined by the mixture of εs to εd partial waves, it is unlikely that this mixture will change much from photoline to photoline, particularly since the incident photon energy is relatively far above threshold. It should be noted that, while the relative variation in the β values from peak to peak is likely to be of high accuracy, the absolute values may have an uncertainty greater than that indicated in Table I (statistical only), where the absolute β values could be lower by as much as 0.4 β units.

In conclusion, we have measured and calculated the $2p$ fine-structure dynamics arising from the open-shell character of atomic chlorine. Of the ten predicted thresholds, we observe eight. Binding energies, relative intensities, and β values for all photopeaks have been determined at a photon energy of 245.04(3) eV. Measured values are in reasonably good agreement with our calculations. Present discrepancies between experiment and theory can be partly attributed to the moderate resolution of this experiment. A definitive explanation will require a measurement with improved resolution. With the exception of one peak, β values of the various photopeaks are quite similar, indicating little change in the relative mixture of the εs to εd partial waves.

Finally, it is worth contrasting the inner-shell behavior of this atom with its closed-shell counterpart, argon. In the closed-shell atom inner-shell photoionization leads to a simple well-resolved spin-orbit doublet. However, the open-shell atom leads to a considerable increase in the complexity of the PES, where any definitive indication of the spin-orbit splitting becomes tenuous at best. These results imply the need for caution when using binding energies found in tabulations for the elements in their natural forms [18] or for free atoms [19] when applied to open-shell atoms. In these tabulations, binding energies are given in terms of spin-orbit doublets, even though they have limited relevance for open-shell atoms. For example, in Ref. [18] the binding energies of the Cl-$2p_{3/2,1/2}$ photopeaks are given as 200 and 202 eV, respectively. Not only are there not two photopeaks, but the thresholds are spread over more than 5 eV. This result is likely to be the general case for shallow core levels. However, for deep core levels the spin-orbit splitting will become sufficiently large, such that any multiplet splitting arising from the open-shell nature of the atom will be superimposed on each spin-orbit doublet. Hence, for this regime, the tabulated spin-orbit binding energies may serve as a rough estimate of the actual atomic structure.

This work was supported by an internal research grant from the University of Wisconsin–Eau Claire and the National Science Foundation under Grant No. PHY-9507573. The University of Wisconsin SRC is operated under National Science Foundation Grant No. DMR-9531009. Support from the SRC staff is gratefully acknowledged as is a loan of part of the experimental apparatus from Oak Ridge National Laboratory.

[1] M. O. Krause, in *Synchrotron Radiation Research*, edited by H. Winick and S. Doniach (Plenum Press, New York, 1980), Chap. 5, p. 101.
[2] V. Schmidt, Rep. Prog. Phys. **55**, 1483 (1992).
[3] B. Sonntag and P. Zimmermann, Rep. Prog. Phys. **55**, 911 (1992).
[4] *VUV- and Soft X-Ray Photoionization Studies*, edited by U. Becker and D. A. Shirley (Plenum Press, New York, 1996).
[5] L. Journel *et al.*, Phys. Rev. Lett. **76**, 30 (1996); A. Gottwald *et al.*, J. Phys. B **31**, 3875 (1998).
[6] M. O. Krause *et al.*, Phys. Rev. A **47**, 3015 (1993); P. van der Meulen *et al.*, *ibid.* **46**, 2468 (1992); P. van der Meulen *et al.*, J. Phys. B **25**, 97 (1992).
[7] L. Nahon *et al.*, Phys. Scr. **T41**, 104 (1992); L. Nahon and P. Morin, Phys. Rev. A **45**, 2887 (1992).
[8] C. D. Caldwell *et al.*, Phys. Rev. A **59**, R926 (1999).
[9] S. Benzaid *et al.*, Phys. Rev. A **57**, 4420 (1998); S. Benzaid *et al.*, *ibid.* **54**, R2537 (1996); C. D. Caldwell *et al.*, *ibid.* **53**, 1454 (1996); C. D. Caldwell and M. O. Krause, J. Phys. B **27**, 4891 (1994).
[10] M. Bissen *et al.*, Rev. Sci. Instrum. **66**, 2072 (1995).
[11] M. O. Krause *et al.*, Phys. Rev. A **30**, 1316 (1984).
[12] D. A. Shaw *et al.*, J. Phys. B **17**, 1173 (1984).
[13] V. Schmidt *et al.*, Phys. Rev. Lett. **38**, 63 (1977).
[14] S. B. Whitfield *et al.*, J. Phys. B **25**, 4755 (1992).
[15] We do not expect any PCI distortion to be seen in the Cl-$2p$ photopeaks at the present resolution since their natural widths are surprisingly narrow [8]. Furthermore, none is seen in the isolated peaks of the spectra, e.g., peak 7.
[16] R. D. Cowan, *The Theory of Atomic Structure and Spectra* (University of California Press, Berkeley, 1981), esp. Chaps. 8 and 16.
[17] M. H. Chen and B. Crasemann, Phys. Rev. A **10**, 2232 (1974).
[18] G. P. Williams, in *X-Ray Data Booklet*, edited by D. Vaughan (University of California, Berkeley, 1985), Table 2-2; J. A. Bearden and A. F. Burr, Rev. Mod. Phys. **39**, 125 (1967).
[19] W. Lotz, J. Opt. Soc. Am. **60**, 206 (1970).